

Estimation of seismic energy released by snow avalanches

Author: Marc Fisse Roselló

*Facultat de Física, Universitat de Barcelona, Diagonal 645, 08028 Barcelona, Spain.**

Abstract: The use of seismic signals created by an avalanche allow us to get many details of it, such as its type (powder, wet or transitional), its velocity or an estimation of its released seismic energy or size. In this work an analysis on the frequency distribution, the velocity and duration of the signals is used to estimate the energy of three avalanches of different types (powder snow, transitional and wet snow) artificially provoked in the Vallée de La Sionne (Switzerland). The seismic signals were recorded by the instrumentation of the avalanche group of University of Barcelona.

I. INTRODUCTION

The study of avalanches has been a topic for a long time, principally to minimize the damages that they can cause to buildings and population. But it was not until a few decades ago that a new method was presented. This new method is based on the study of the seismic signal left from an avalanche at its path ([1], [2], [3], [4]). An important research in this new methodology was carried out by the Avalanche Group RISKMAT of the University of Barcelona in the last years. The estimation of the energy released by an avalanche is one of the subjects of this research.

Most of the avalanches used for this research were artificially released in Ryggfonn (Norway) and in Vallée de La Sionne (VdLS) (Switzerland). The data of these avalanches were recorded by two (Ryggfonn) or four (VdLS) three-component wide-range seismometers located in the avalanche path or near it.

The data used for this work are from three avalanches that took place in VdLS. FIG. 1 shows a profile of the path that followed the avalanches used. The horizontal distance covered by the avalanches was about 2300m with approximately 1000m from the highest point to the lowest one. In the FIG. 1 the caverns for the sensors are marked with A, B, C, and D. Only the data recorded in the caverns B and C were used since all three avalanches were released between before cavern B, and none of them was large enough to reach cavern D, that, in this case, recorded only the infrasound (which, despite being an interesting phenomena is not matter of study in this work).

For the study of the avalanches the subsequent steps are followed:

1. First, a frequency analysis (spectra and spectrogram) is done, given that in previous studies ([5]) was demonstrated that it is a good method to distinguish the type of avalanche.
2. Secondly we will focus on the avalanche velocities. This is a crucial property to study, since all the

data recorded are in the time domain and to use eq. (1) the distance is needed.

3. Later on, a study of the envelopes of the avalanches signals was made. Since the energy released by an avalanche depends on the squared envelope this study should give us a lot of information of the energy distribution of the avalanche.
4. Finally, once all previous items are known, the energy of the three avalanches will be calculated.

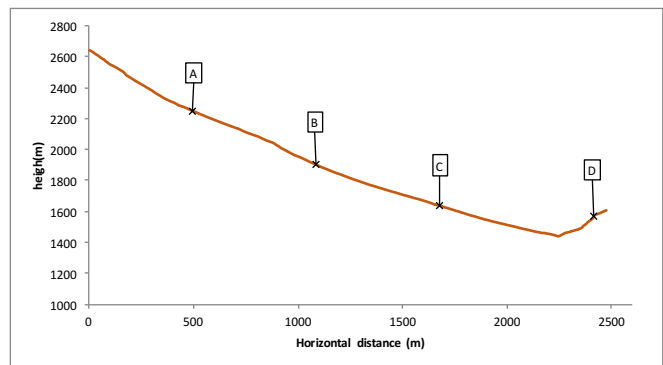


FIG. 1: Path followed by the avalanches with the horizontal and vertical distances in meters from DTM (digital topographic model).

To fully determine the energy of an avalanche one must calculate the eq. (1) ([2], [6]):

$$E = \int_{t_1}^{t_2} \int_{f_1}^{f_2} \rho c(f) A^2(f, t) 2\pi r(t) h(f) e^{\frac{2\pi f r(t)}{Q(f)c(f)}} df dt \quad (1)$$

In this equation the energy decay with time is assumed to be produced by geometrical spreading of the wave and intrinsic attenuation of the amplitude with distance. This equation corresponds to the recovering of the energy released. ρ is the ground density, $c(f)$ the phase velocity of the seismic surface waves, $A(f, t)$ the amplitude of the ground motion (m/s) (measured with the sensors in the three components), $r(t)$ the avalanche front-seismometer distance, $h(f)$ corresponds to $\frac{1}{4}$ of the wave length, $Q(f)$ is the Quality factor and f the frequency. Q , c and ρ , depending on the ground characteristics. The $2\pi r(t)h(f)$

*Electronic address: mrc.fisse@gmail.com

factor appears due to the propagation model of the wavefront that is considered to be cylindrical (it corresponds to the area of a cylinder of radius r and depth h) ([2]).

In this work we are interested in calculating the energy, in consequence, the focus is on determining and analysing the $A(f, t)$ parameter, to calculate $A^2(f, t)$. The other ones were previously calculated by the research team commented before, with the data obtained in VdLS.

II. DATA ANALYSIS

A. Frequency analysis

The seismic data obtained from the avalanches are the amplitude of the ground motion (m/s) in the three components (East-West, North-South and the vertical, Z) for each cavern at a rate of 100Hz (FIG. 2). The three avalanches used for this study are the #3019, a transitional large avalanche, the #3020, a wet large avalanche and the #3024, a powder medium size avalanche. As an example, FIG. 2 shows the time series of the N-S component (left) and the corresponding frequency distribution (right) obtained at cavern B placed in the middle of the path. To obtain the frequency distribution the *Fast Fourier Transform* (fft function of the "numpy" library in python) was used, and for the representation the absolute value was calculated and normalized. We observe a different behaviour of the time series and of the frequency content. One can observe that the wet (#3020) avalanche has most part of the energy on the high frequencies (>10Hz), the transitional avalanche (#3019) seems to have a pick in low frequencies and most of the energy in high frequencies and, finally, the powder avalanche (#3024) has the major part of the energy is on the frequencies below 10Hz. These are in line of that found in [5].

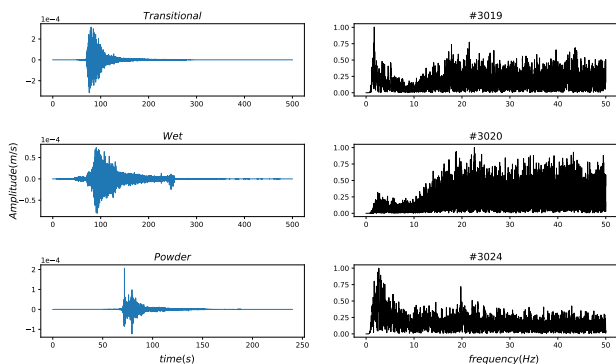


FIG. 2: Representation of data obtained for N-S component in cavern B. On the left the representation of the amplitude of the ground motion (m/s) from each avalanche is presented and on the right we find the absolute value for normalized Fourier Transform of three avalanches is presented.

As regards the spectrogram, the evolution of the frequency content in time is presented in FIG. 3(a). For the lack of space, only spectrograms of the N-S component of the wet avalanche in B and C caverns are presented.

We define the sections, front, body and tail as the signal received before the avalanche reaches the sensor, the signal when the avalanche is over the sensor and finally the signal received once the avalanche passed the sensor respectively (indicated on FIG. 3(a)) ([5]). In cavern B, we can observe that while in the body of the wet avalanche the frequencies distribution is quite uniform, the tail of the avalanche has its major part of energy on frequencies higher than 15Hz (see FIG. 3(a)). The reason of this is because of the composition of the snow. The body part of a wet avalanche have compact dense snow that moves uniformly through the slope generating low frequency signals, but on the tail high frequency vibrations are generated due to the rapid density and pressure fluctuations in the low part of the avalanche. In order to save space no spectrogram for the powder avalanche is presented, but the same phenomena is observed on the tail region for powder avalanches, where rapid pressures fluctuations create high frequency vibrations (and then, high frequency signals are measured) ([5]).

In the cavern C (FIG. 3(a) bottom) we can observe that low frequency signals are received when the avalanche front gets the cavern B (FIG. 3(a) top) while high frequencies are only received when the avalanche body gets to the cavern. The justification for this behaviour is found on the eq. (1): the exponential of this equation corresponds to an attenuation factor, and as it is easy to see, it depends on the frequency; at higher frequency the higher the attenuation, causing frequencies above 15Hz to attenuate before reaching cavern C.

Because it is necessary to transform the time to distance to use the Eq.(1), velocities are calculated and analysed.

B. Velocity analysis

Front average velocities between cavern B and C were obtained by considering the distances of the sensors, and the arrival time of the avalanche to these. The velocities of the different avalanches were calculated with a script written in python. The coordinates of the path of the avalanches were used to draw the slope and to calculate the velocity; the coordinates of the caverns were also known, making easy to place them on the path. The distance between caverns was calculated using the Pythagoras Theorem using the UTM coordinates. The time that took the front of the avalanche to travel from cavern B to cavern C was obtained with the help of the spectrograms. The picking for the instant when the avalanche passes over the selected cavern was done manually amplifying the images of the spectrograms, corresponding to the beginning of the body section.

The front average velocities estimated for the three

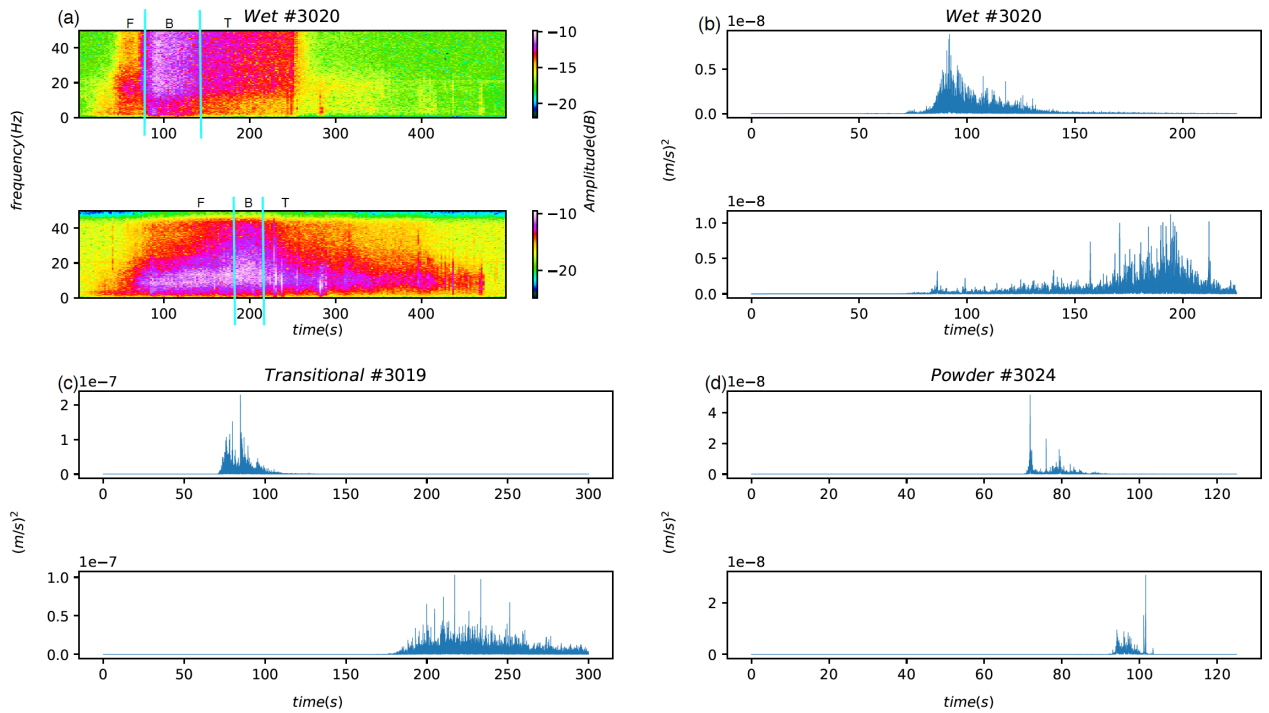


FIG. 3: (a): Spectrograms of B (top) and C (bottom) caverns of the wet avalanche; front (F), body (B) and tail (T) parts are pointed out in each spectrogram. Signals envelopes for both caverns (B on top and C on bottom) for each avalanche: (b) wet avalanche, (c) transitional avalanche and (d) powder avalanche. For lack of space no more spectrograms are shown in this figure.

avalanches between B and C were 6.40 ± 0.15 m/s, 6.15 ± 0.09 m/s and 27.9 ± 0.6 m/s for transitional (#3019), wet (#3020) and powder (#3024) avalanche respectively. These values are in agreement with the ones obtained in 2007 by [3], that stated that avalanche velocities are between 5 m/s and 70 m/s, with low values for wet/transitional avalanches in general and high values for powder ones.

The velocities of the wet and transitional avalanches are practically identical. Because the transitional avalanche is supposed to be partially a powder avalanche one would expect to be faster than a wet one. However, there is a good justification for this; the signals observed are seismic signals, generated for the part of the avalanche in contact with the ground. In a transitional avalanche we have some powder (lighter) snow and some wet (denser) snow, so the wet part is the one that is in contact with the ground and the one which generates the seismic signals ([5]).

C. Envelope analysis

Since the energy of an avalanche depends on the amplitude of the signal, the envelope area should give us quite information about the avalanche energy. To calculate the envelopes area the following python tools were used: *simps* integration and the *trapz* integration on

the “scipy.integrate” and “numpy” libraries, respectively. The first one uses the trapezoidal rule and the second one the Simpson’s rule to integrate the area below a curve. The final result considered for the area (Table I) is the arithmetic median between the two values obtained.

We are interested in the different contributions to the energy of the sections. To this end, to distinguish and analyse separately the different contributions of the parts, the area of the squared envelope of different parts was calculated. The parts considered are, as commented before, the front, the body and the tail.

We can observe that, in general, the tail is the longest part in all the avalanche types, but the body is the part with the highest squared envelopes areas (see Table I) and so, the most energetic part (Eq. (1)). This is what one would expect since it is the most violent part of the avalanche. Table I also shows that the areas of the three parts of the wet avalanche are similar, indicating that the energy released is similar (Eq. (1)). This is not the case with the transition and powder avalanches where there are significant differences in the three parts.

One thing to keep in mind is that powder avalanches are characterized by having a considerable part of their snow floating in the air. This can make this method underestimate the envelope amplitude (and hence, the energy) of powder avalanches, since the snow floating in the air would not create any seismic signal. This fact was already seen in [7].

Cavern	#3019 Trans		#3020 Wet		#3024 Pow	
	B	C	B	C	B	C
Front Area (m^2/s)	$4.498 \cdot 10^{-11}$	$1.299 \cdot 10^{-9}$	$2.076 \cdot 10^{-10}$	$1.809 \cdot 10^{-8}$	$1.694 \cdot 10^{-11}$	$2.071 \cdot 10^{-10}$
t_{front} (s)	5	101	29	105	10	42
Body Area (m^2/s)	$3.180 \cdot 10^{-7}$	$5.588 \cdot 10^{-7}$	$2.579 \cdot 10^{-8}$	$6.127 \cdot 10^{-8}$	$1.890 \cdot 10^{-8}$	$1.161 \cdot 10^{-8}$
t_{body} (s)	50	141	52	75	25	16
Tail Area (m^2/s)	$6.415 \cdot 10^{-9}$	$4.084 \cdot 10^{-9}$	$4.301 \cdot 10^{-9}$	$1.274 \cdot 10^{-8}$	$6.908 \cdot 10^{-10}$	$4.289 \cdot 10^{-11}$
t_{tail} (s)	150	110	125	247	55	82

TABLE I: Areas obtained of the squared envelope of the different parts of the avalanches and duration of each part.

III. ENERGY CALCULATION

The energy released by an avalanche in a certain point decays with distance because of two effects ([2]):

1. The anelastic attenuation (an exponential decay of the energy with distance).
2. The geometrical spreading (a proportional decay of the energy with distance due to the cylindrical propagation model considered)

Eq. (1) allows us to recover the energy generated on a previous point from the location of our sensor.

Using the signals obtained in cavern B we can obtain the total energy released by the avalanche in the previous moments to arrive to this sensor. For C cavern the procedure is the same. The data at that point considers all the time before the avalanche reached cavern B and all the time that took the avalanche to cover the distance between the B and C cavern.

As shown in FIG. 3 the envelopes of the three avalanches show some picks of amplitude in certain points. The reason of this could be energy noise due to rolling stones or ice that hit the sensor. In order to not overestimate the energy from the avalanches an attenuation of the points where the envelopes presented isolated picks long before the avalanches reached cavern was made, since at these points it is reasonable to consider that picks of energy are caused by noise.

The energy obtained for each avalanche is shown in the Table II:

	#3019 Trans	#3020 Wet	#3024 Pow
Cavern B (J)	476	$4.93 \cdot 10^5$	$3.24 \cdot 10^3$
Cavern C (J)	$1.88 \cdot 10^7$	$1.03 \cdot 10^9$	$1.06 \cdot 10^6$

TABLE II: Energy released by each avalanche before reaching caverns B and C.

As expected, the powder avalanche is the less energetic, followed by the transitional one and finally, the wet avalanche is the one with most energy.

It is important to emphasize that the energy obtained using eq. (1) corresponds to the energy released by each avalanche before reaching the sensor. Eq. (1) does not

allow us to calculate the energy of the avalanche when it is passing through over the sensor, since, in that moment the distance between avalanche and sensor would be zero, and the energy obtained using eq. (1) would be also zero. So, eq. (1) allows us to calculate the total energy received on a cavern but only the envelope analysis allows us to obtain an estimation of the distribution of this energy in the different parts of the avalanche.

Integrating eq. (1) only in the frequencies we can get the time distribution of the energy of an avalanche and, using the velocity of that avalanche we can transform this time distribution of the energy to distance distribution, which can be useful for further studies. These results are shown in FIG. 4 and FIG. 5, where the plot of the energy released by all three avalanches in every position before reaching cavern B and C respectively are shown. We can observe that the transitional avalanche started practically over the sensor, being slight the energy released before that point. In opposition, wet and powder avalanches started quite far from the B cavern, being the energy released before reaching it higher.

Also, for the powder avalanche the seismic energy that reached cavern C was very low, making it impossible to recover the energy released at points farther than 400m from cavern C (FIG. 5). As commented in [7] and in the previous section, the reason of this is that a significant part of the snow moved by a powder avalanche is not in contact with the ground and hence, it does not create any seismic signal.

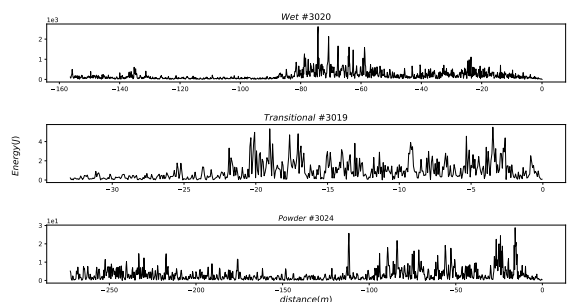


FIG. 4: Representation of the energy released in every position by each avalanche before reaching cavern B (distance = 0). On the horizontal axis the distance from the point to B is represented.

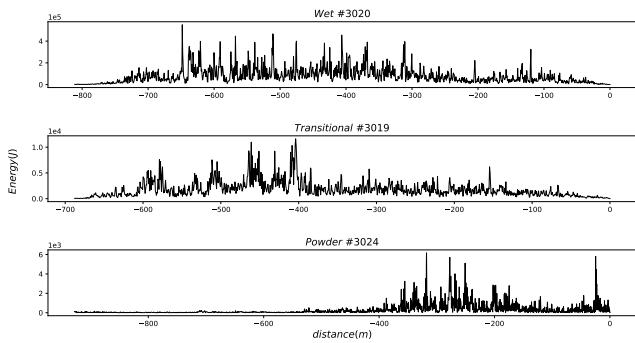


FIG. 5: Representation of the energy released in every position by each avalanche before reaching cavern C (distance = 0). On the horizontal axis the distance from the point to C is represented.

IV. CONCLUSIONS

The method presented, with the current distribution of the equipment along the path, seems to be a good way to study the seismic energy released by transitional and wet avalanches, since it requires no risk for the obtaining of data and the only need to treat these data is a computer and few programming skills and the results obtained were satisfactory. Also it permits to study the energy distribution in the different parts of the avalanche in a very simple way (as seen in the envelope analysis). In addition, the steps to follow for obtaining and processing data using this method is quite easy (the sensors can be left there until it is necessary to get the data) and reasonably cheap (the only expenses would be on

the instrumentation used, and on the transport to get the location of study).

While this method seems to give quite good results it would be interesting, if there is the possibility, to use others complementary methods to calculate for example the velocity of the avalanches (as presented in [5], where radar data were used to calculate the velocity of avalanches). Since powder and transitional avalanches are characterized for having part of the transported snow in form of floating particles, this part of the avalanche would not generate any seismic signal. As seen in [7] and in this work, this fact can also make this method to underestimate the energy of powder and transitional avalanches. To confirm this would be interesting to develop further studies comparing the energy calculated using this method and different ones. Another failure of this method could be that the data recorded are very sensitive to noise with sources in moving objects that can hit the sensor and, in some cases, it is difficult to distinguish noise from the real signal. However, this can be solved by analysing the spectrograms. With further studies on the method it would be able to improve some of its weak points and eventually become a major method to determine avalanches energy.

V. ACKNOWLEDGEMENTS

First of all I would like to thank my advisor Dr. Emma Suriñach Cornet for her guidance and help with all the clarifications needed in every moment. Thanks also to my friends and family who supported me in every moment and helped me with their advises.

-
- [1] C. Pérez Guillén, B. Sovilla, E. Suriñach, M. Tapia, A. Köhler (2016). *Deducing avalanche size and flow regimes from seismic measurements*. Cold Regions and Technology 121, 25-41.
- [2] I.Vilajosana, E. Suriñach, G. Khazaradze, P. Gauer (2007). *Snow avalanche energy estimation from seismic signal analysis*. Cold Regions and Technology 50, 72-85.
- [3] I.Vilajosana, G. Khazaradze, E. Suriñach, E. Lied, K. Kristensen (2007). *Snow avalanche speed determination using seismic methods*. Cold Regions and Technology 49, 2-10.
- [4] A. Kogelnig, E. Suriñach, I. Vilajosana, J. Hübl, B. Sovilla, M. Hiller and F. Dufour (2011). *On the complementarity of infrasound and seismic sensors for monitoring snow avalanches*. Natural Hazards and Earth System Sciences, 11,2355-2370,2011.
- [5] Pérez Guillén, C. (2016). *Advanced seismic methods applied to the study of snow avalanche dynamics and avalanche formation*. PhD thesis, Universitat de Barcelona.
- [6] Suwa, H., Akamatsu, J., Nigai Y. (2003). *Energy radiation by elastic waves on debris flows*. *Debris Flows Hazard Mitigation: Mechanics, Prediction and Assessment*. Millpress, Rotterdam.
- [7] Biescas, B. (2003). *Aplicación de la sismología al estudio y detección de aludes de nieve*. PhD thesis, Universitat de Barcelona.